Article

V. Ramanathan

Trace-Gas Greenhouse Effect and Global Warming

Underlying Principles and Outstanding Issues

Volvo Environmental Prize Lecture-1997

This paper describes the developments that transformed the global warming problem from that arising solely from CO_2 increase to the trace-gas greenhouse effect problem in which several non-CO_2 gases, CFCs, CH_4, N_2O, O_3 and others contribute as much as CO_2. Observed trace-gas increases, including CO_2 increase, since the mid-19th century have enhanced the atmospheric greenhouse effect, G_a, ($\approx 130 \pm 5$ W m^{-2}) by about 2%. Without other competing factors, this heating should have committed the planet to a warming of about 1 to 1.5 K. The added radiative energy is maximum in the low latitudes and about a factor of two smaller in the polar regions. The largest effect of the warming is increased back radiation at the surface by as much as 6 to 8 W m^{-2} per degree warming. Not all of this increased energy is balanced by surface emission; evaporation (and hence precipitation) increases to restore surface energy balance, by as much as 2 to 4% per degree warming. The increase in evaporation along with the increase in saturation vapor pressure of the warmer troposphere, contributes through the atmospheric dynamics to an increase in water vapor. This water vapor feedback enhances G_a by another 1% per degree warming. Our ability to predict regional and transient effects, depends critically on resolving a number of outstanding issues, including: *i)* Aerosol and stratospheric ozone effects; *ii)* Response of the tropical convective-cirrus clouds, the extra-tropical storm-track systems and persistent coastal stratus to both global warming and to regional emissions of aerosols; *iii)* The causes of excess solar absorption in clouds; and *iv)* Upper troposphere water vapor feedback effects.

INTRODUCTION

From Fourier and Arrhenius to IPCC (1): The mathematician Baron Jean-Baptiste Fourier (2) suggested in the year 1827, that the atmosphere behaves like the transparent glass cover of a box exposed to the sun by allowing sunlight to penetrate to the Earth's surface and retaining the longwave radiation ("obscure radiation") from the Earth's surface. This inference is perhaps one of the earliest suggestions of the greenhouse effect of the atmosphere. By about the mid-19th century, the pyrheliometric observation of Pouillet (3) and the ingenious laboratory experiments of Tyndall (4) demonstrated the selective spectral absorption of longwave radiation by atmospheric H_2O and CO_2.

Accurate atmospheric solar and infrared (IR) transmission observations were needed to extrapolate laboratory data to atmospheric conditions and construct greenhouse models of the atmosphere. Langley (5) invented the bolometer radiometer to fill the void. Langley's accurate observations of lunar and solar spectra and the correct identification of numerous H_2O and CO_2 absorption bands set the stage for a new milestone in greenhouse-effect studies, which was the model for the surface-atmosphere radiation budget and temperature change developed by Arrhenius (6) in the year 1896.

The successes of Arrhenius' model are many (7), including the accurate simulation of the total emissivity of the atmosphere, simulating the logarithmic dependence of the CO_2 greenhouse effect and the inclusion of the water vapor feedback by invoking the constant relative humidity assumption. The result, that a doubling of CO_2 would warm the globe significantly, enabled Arrhenius (7) and later Chamberlin (8), to resurrect an earlier unpublished suggestion by Tyndall that the past glacial epochs may be due to a reduction in atmospheric CO_2 by a factor of about 2. Studies aimed at relating CO_2 variation to surface warming received significant impetus with the publication of Callendar's paper (9) in the late 1930s, which concluded that atmospheric CO_2 concentration began increasing due to fossil fuel combustion since the 1900s, and this increase would warm the globe by about 0.03°C per decade.

The greenhouse theory of climate change underwent a significant refinement and took its modern shape with the publication of the Manabe and Wetherald (10) paper, which convincingly demonstrated that the CO_2-induced surface warming is not solely determined by the energy balance at the surface but by the energy balance of the coupled surface-troposphere-stratosphere system. The underlying concept of the Manabe-Wetherald model (see review in (11)) is that the surface and the troposphere are so strongly coupled by convective heat and moisture transport that the relevant forcing governing surface warming is the net radiative perturbation at the tropopause, simply known as radiative forcing (1).

This theory also elevated the importance of the stratosphere to climate. For example, it became possible for decreases in lower stratospheric ozone, through decreased downward emission from the cooler stratosphere, to cool the upper troposphere and through convective coupling, induce a surface cooling (12). The radiative-convective theory was confirmed by general circulation climate models, GCMs, and has become an important analytical tool for interpreting GCMs (13, 14).

The next important development arose from a flurry of new findings in the 1970s and 1980 on the greenhouse effect of trace gases, which were largely prompted by new discoveries in atmospheric chemistry of the stratospheric ozone layer (15, 16).

First, was the demonstration in 1975 (17) that CFCs have a direct greenhouse effect and that the surface warming effect of $CFCl_3$ (CFC-11), and CF_2Cl_2 (CFC-12), was significantly (about 10 000 times or more) greater than that of CO_2 increase on a molecule per molecule basis. This study was motivated by Molina and Rowland's paper (15) on the role of CFCs in stratospheric ozone depletion. CH_4 and N_2O (18) were immediately (in 1976) added to the list of greenhouse gases, since their concentrations were shown to be increasing. In addition, CH_4 and N_2O, which were not included in any climate models, were shown to contribute as much as 2K to the present climate (19). The list grew eventually to several tens of greenhouse gases (see Table 1 from Ramanathan et al. (20)). Prompted by Crutzen's (15) paper on the role of nitrogen oxides on stratospheric ozone, it was shown in 1976 (12) that decreases in stratospheric ozone can lead to surface cooling. A few years later, tropospheric ozone emerged as an important greenhouse gas (21, 22), since it was recognized that tropospheric ozone can increase due to oxidation of pollutants such as CO and CH_4 (e.g., 22).

The above developments, over a period of a few years, set the

stage for a number of studies estimating the climate change due to the observed trace gas increases (e.g. 20, 23–26), which culminated in a comprehensive WMO sponsored assessment report on the role of non-CO_2 trace gases in 1985 (27). This report concluded that the problem concerning the greenhouse effects of human activities has broadened in scope from the CO_2-climate problem to the trace-gas climate problem, and that for the post-1960 time period, non-CO_2 trace gas forcing has equalled the greenhouse effect of CO_2, thus significantly accelerating the warming.

In the meantime, the convincing demonstration of the CO_2 increase through the so-called *Keeling curve* (28) and the GCM simulation of CO_2 global warming of about 4 K (13, 14), made it clear by the mid-1980s that serious policy options to regulate the increase of greenhouse gases must be explored. The global nature of the problem demanded an international consensus and the unprecedented Intergovernmental Panel on Climate Change (IPCC) was established in the late 1980s under the chairmanship of B. Bolin. The IPCC reports (1) essentially confirmed the earlier findings on the importance of trace gases. But, other surprising developments were unfolding.

- The first development concerns the observed Antarctic ozone hole. The global-wide depletion of lower stratospheric ozone observed since the late 1970s, was estimated to have a potentially large radiative cooling of the surface-troposphere system (29).
- The next development was the culmination of several decades of study of the aerosol cooling effect in the Charlson et al. (30) paper, which established that the potential radiative cooling effect of anthropogenic sulfate aerosols may be a third or half as large as the CO_2 radiative forcing. The complex regional nature of the forcing, was even more surprising (31). The effect of smoke aerosols from biomass burning in regions such as the Amazon (32) was added to the list.
- Lastly, analyses (33, 34) of the Earth Radiation Budget Experiment (ERBE) satellite revealed that clouds caused a large net radiative cooling of the earth. In parallel, a comprehensive study (35) that compared 19 GCMs revealed large differences in climate model predictions of cloud feedbacks in GCMs. These developments confirmed that cloud feedback is a Gordian knot of the climate prediction problem.

The main focus of this paper is on the radiative forcing and feedbacks that are the starting point of models of global warming. Atmospheric and ocean dynamics play equally important roles in global warming, a detailed discussion of which can be found in IPCC (1) and Bengtsson (36).

UNDERLYING PHYSICAL PRINCIPLES

It is convenient to separate the greenhouse effect from global warming. The former is based on observations and physical laws such as Planck's law for black-body emission. The concept of warming that results from the greenhouse effect, is based on deductions from sound physical principles. Numerous feedback processes, determine the magnitude of the warming; these feedbacks are treated with varying degrees of sophistication in

Table 1. Estimates of the abundance of trace chemicals in the global atmosphere of 1980.

Chemical Group	Chemical Formula	Dominant Source*	Dominant Sink*	Year 1980 Global Average Mixing Ratio, ppb†	Remarks (also see text for details)
Carbon dioxide	CO_2	N,A	O	339 x 10^3	**Fossil fuel combustion**
Nitrogen compounds	N_2O	N,A	S(UV)	300	Combustion and fertilizer sources
	NH_3	N,A	T	< 1	Concentration variable and poorly characterized
	($NO + NO_2$)	N,A	T(OH)	0.05	Concentration variable and poorly characterized
Sulfur compounds	CSO	N,A	T(O,OH)?	0.52	
	CS_2	N,A	T	< 0.005	
	SO_2	A(?)	T(OH)	0.1	
	H_2S	N	T(OH)	< 0.05	
Fully fluorinated species	CF_4	A	I	0.07	Aluminum industry a major source
	C_2F_6 (CFC16)	A	I	0.004	Aluminum industry a major source
	SF_6	A	I	0.001	
Chlorofluoro-carbons	$CCIF_3$ (CFCI3)	A	S(UV),I	0.007	All chlorofluorocarbons are of exclusive man-made origin. A number of regulatory actions are pending. The nature of regulations and their effectiveness would greatly affect the growth of these chemicals over the next 50 years.
	CCl_2F_2 (CFC12)		S(UV)	0.28	
	$CHCIF_2$ (CFC22)	A	T(OH)	0.06	
	CCl_3F (CFC11)	A	S(UV)	0.18	
	CF_3CF_2Cl (CFC115)	A	S(UV)	0.005	
	$CCIF_2CCIF_2$ (CFCII4)	A	S(UV)	0.015	
	CCl_2FCCIF_2 (CFCII3)	A	S(UV)	0.025	
Chlorocarbons	CH_3Cl	N(O)	T(OH)	0.6	Dominant natural chlorine carrier of oceanic origin
	CH_2Cl_2	A	T(OH)	0.03	A popular reactive but nontoxic solvent
	$CHCl_3$	A	T(OH)	0.01	Used for manufacture of F22; many secondary sources also exist
	CCl_4	A	S(UV)	0.13	Used in manufacture of fluorocarbons; many other applications as well
	CH_2ClCH_2Cl	A	T(OH)	0.03	A major chemical intermediate (global production = 10 tg/yr); possibly toxic
	CH_3CCl_3	A	T(OH)	0.14	Nontoxic, largely uncontrolled degreasing solvent
	C_2HCl_3	A	T(OH)	0.005	Possibly toxic, declining markets because of substitution to CH_3CCl_3
	C_2Cl_4	A	T(OH)	0.03	Possibly toxic, moderate growth due to substitution to CH_3CCl_3
Brominated and iodated species	CH_3Br	N	T(OH)	0.01	Major natural bromine carrier
	$CBrF_3$	A	S(UV)	0.001	Fire extinguisher
	CH_2BrCH_2Br	A	T(OH)	0.002	Major gasoline additive for lead scavenging; also a fumigant
	CH_3I	N	T(UV)	0.002	Exclusively of oceanic origin
Hydrocarbons, CO, H_2	CH_4	N	T(OH)	1650	**Increasing cattle population and cultivation**
	C_2H_6	N	T(OH)	0.8	Predominantly of auto exhaust origin
	C_2H_2	A	T(OH)	0.06	No trend has been identified to date
	C_3H_8	N,	T(OH)	0.05	No trend has been identified to date
	CO	N,A	T(OH)	90	No trend has been identified to date
	H_2	N,A	T(SL,OH)	560	
Ozone	O_3 (Tropospheric)	N	T(UV, SL,O)	$F(Z)^+_+$	**Trend appears to exist but data are insufficient**
Aldehydes	HCHO	N	T(OH,UV)	0.2	Secondary products of hydrocarbon oxidation
	CH_3CHO	N	T(OH,UV)	0.02	

* N, naturall; A, anthropogenic; O, oceanic; S, stratosphere; UV, ultraviolet photolysis; T, troposphere; OH, hydroxyl radical removal; I, ionospheric and extreme UV and electron capture removal; SL, soil sink.
† These concentrations are integrated averages; for chemicals with lifetimes of 10 years or less, significant latitudinal gradients can be expected in the troposphere; for chemicals with extremely short lifetimes (0.001–0.3 years) vertical gradients may also be encountered.
$^+_+$ Varies from 25 ppbv at the surface to about 70 ppbv at 9 km. The concentration was increased uniformly by the same percentage from the surface to 9 km.
Source: Adapted from Ramanathan et al. (20).

GCMs and other climate models. As a result, predictions of the magnitude of the warming are not only model dependent but also are subject to large uncertainties. The physics of the greenhouse effect is described first, followed by the deduction that a global warming has to result from an enhancement of the greenhouse effect. The role of the feedbacks is explained last.

Greenhouse Effect

Global energy budget: The greenhouse effect is best illustrated from the annual and global average radiative energy budget. The incoming solar radiation, the reflected solar radiation and the outgoing longwave radiation (OLR) to space (Fig. 1) at the top of the atmosphere have been determined by satellite measurements. The OLR is contained in wavelengths longer than 4 μm and is referred to here as longwave or infrared (IR) radiation.

Globally, 70% of the incoming solar radiation is absorbed by the earth-atmosphere system. The solar absorption heats the system, and the surface-atmosphere system cools by emitting OLR until it balances the absorbed solar radiation of 237 W m^{-2}. Climate models are based on this fundamental principle of global radiation energy balance.

Reduction in OLR: At a global average surface temperature of about 289 K, the globally averaged longwave emission by the surface is about 395 ± 5 W m^{-2}, whereas the OLR is only 237 ± 3 W m^{-2} (Fig. 1). Thus, the intervening atmosphere and clouds cause a reduction of 158 ± 7 W m^{-2} in the longwave emission to space, which is the magnitude of the total greenhouse effect (denoted by G) in energy units. Without this effect the planet would be colder by as much as 33 K.

As shown later, clouds contribute about 30 W m^{-2} to G. About 90% of the balance (≈ 130 W m^{-2}), denoted by G_a for atmospheric greenhouse effect, is due to H_2O and CO_2. The remaining 10% is due to O_3, CH_4, N_2O and CFCs. The ability of these gases to reduce the longwave energy escaping to space has been demonstrated clearly by satellite measurements as shown in Figure 2 (37). The upper boundary of the shaded region in Figure 2 is the emission by the ocean surface, radiating at a temperature of 300 K, whereas the lower boundary is the radiation measured at satellite altitudes; the difference is the net energy absorbed within the atmosphere. CO_2 contributes to the absorption features between 13 to 17 μm; Ozone between 9 and 10 μm and water vapor in the entire spectrum.

Why does the presence of gases reduce OLR? These gases absorb the longwave radiation emitted by the surface of the earth and re-emit it to space at the colder atmospheric temperatures. Since the emission increases with temperature, the absorbed energy is much larger than the emitted energy, leading to a net trapping of longwave photons in the atmosphere. The fundamental cause for this trapping is that the surface is warmer than the atmosphere; by the same reasoning decrease of temperature with altitude also contributes to the trapping since radiation emitted by the warmer lower layers are trapped in the regions above.

Anthropogenic Enhancement of the Greenhouse Effect

By deduction (from the facts inferred above from Figures 1 and 2), an increase in a greenhouse gas such as CO_2 will lead to a further reduction in OLR. If the solar absorption remains the same, there will be a net heating of the planet.

Global Warming

How will the planet restore global energy balance? The surface-troposphere system should warm (in response to the excess energy) and radiate more longwave radiation to space until the OLR emission to space balances the absorbed solar radiation, i.e., the increase in OLR from the warming compensates for the reduction in OLR due to the trace-gas increase. This is the underlying theory behind global warming. It relies on the fundamental Planck's law that the electromagnetic energy emitted by any body in local thermodynamic equilibrium increases with its temperature; the functional form of the increase is given by the so-called Planck function.

Magnitude of the Surface Warming: The Case of CO_2 Doubling

To illustrate the processes that determine the magnitude, we will perform a thought experiment of a doubling of the CO_2 concentration, at say, time $t = t_0$. The approach and the results (Fig. 3) described below follow closely the study by Ramanathan (38). The system is initially in global energy balance before t_0, such that $Q(t < t_0) = 0.0$, where Q = S-F, S is the absorbed solar energy by the surface-troposphere system and F is the net (up minus down flux) longwave emission at the tropopause.

Principles of radiative convective adjustment are invoked to

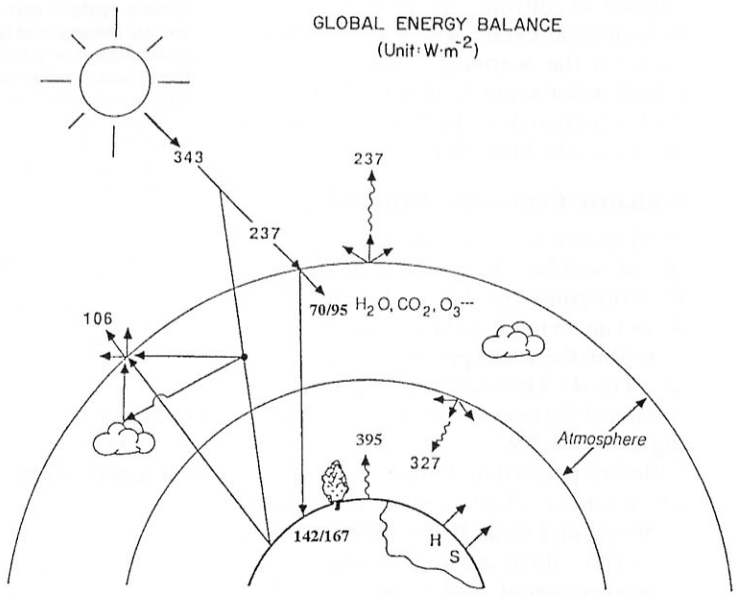

Figure 1. The global energy balance for annual mean conditions. The top of the atmosphere estimates of solar insolation (343 ± 2 W m^{-2}), reflected solar radiation (106 ± 3 W m^{-2}), and outgoing longwave radiation (237 ± 3 W m^{-2}) are obtained from satellite data. The other quantities include atmospheric absorption of solar radiation (in the range of 70 to 95 W m^{-2}); surface absorption of solar radiation (in the range of 142 to 167 W m^{-2}) downward longwave emission by the atmosphere (327 ± 15 W m^{-2}); upward longwave emission by the surface (390 ± 15 W m^{-2}); and H the latent, and S the sensible, heat fluxes from the surface.

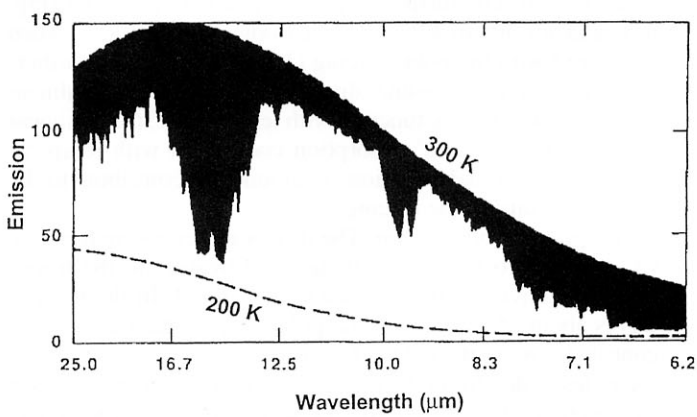

Figure 2. Sample spectra from the infrared interferometer spectrometer onboard Nimbus 3 satellite. The dashed lines indicate the outgoing longwave blackbody emission at the temperatures indicated. Emission is measured in arbitrary units. The scene is tropical Pacific Ocean under clear-sky conditions. (Adapted from (37)).

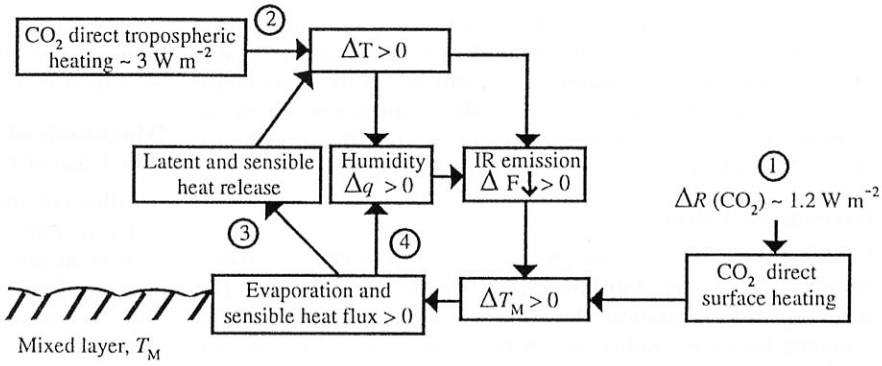

Figure 3. Schematic of the H_2O feedback involving ocean-atmosphere thermal interactions. This is the dominant mechanism by which the greenhouse feedback warms the surface. Abbreviations: *T*, troposphere temperature; T_M, mixed layer temperature; *F*↓, downward infrared emission; *q*, specific humidity; and *R*, the radiative (IR plus solar) flux change at the surface due only to change in CO_2. Values correspond to doubling of CO_2. Numbers within circles designate the feedback loops. Adapted from Ramanathan (38).

explain how feedbacks govern the magnitude of the warming. The global energy balance is reconciled with surface energy balance to illustrate the response of the hydrological cycle, which in turn feeds back on the warming through the so-called, water vapor feedback, cloud feedback (discussed in the last section) and snow/ice albedo feedback.

Radiative-Convective Adjustment

(i) Response at t = t_0 : The immediate response will be a reduction in the OLR at the tropopause by about 3.1 W m^{-2} (Fig. 4) and an increase in the downward emission from the stratosphere by about 1.2 W m^{-2} (Fig. 4). The sum of the two is the net forcing at the tropopause; in other words, the instantaneous forcing $Q(t_0) = 4.3$ W m^{-2}.

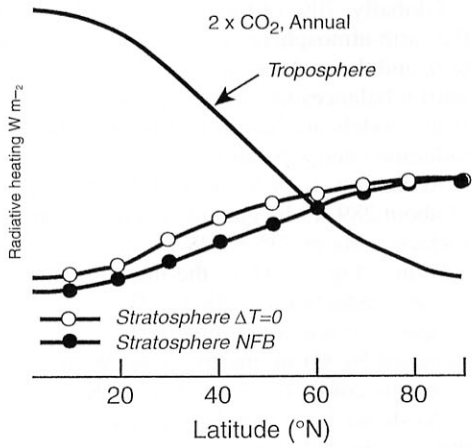

Figure 4. Separate contributions from the troposphere ("TROPOSPHERE" curve) and the stratosphere ("STRATOSPHERE" curve) to the total heating of the surface-troposphere system, due to doubled CO_2, for annual mean conditions. The troposphere contribution is given by the reduction in the upward radiative flux at the tropopause, and the stratosphere contribution is given by the increase in the downward radiative flux from the stratosphere. For the "STRATOSPHERE ΔT=O" curve, stratospheric temperatures are held fixed at the observed value. For the "STRATOSPHERE NFB" curve, stratospheric temperature changes are adjusted from observed values by assuming radiative equilibrium. Source: (40).

Before proceeding further, we will discuss four aspects of the CO_2 forcing to clarify certain misconceptions.

- *Strong and Weak Bands*. Between the four important isotopes of CO_2, there are several tens of strong fundamental and weaker isotopic and excited state absorption bands in the 13 to 18 μm and the 10 μm region. The weak-band radiative forcing increases almost linearly with the CO_2 concentration (39) and the often stated logarithmic dependence of the CO_2 greenhouse effect (IPCC (1)) applies only to the strong bands (39). However, for present day CO_2 levels, the strong bands contribute more than 80% of the forcing and hence the CO_2 total greenhouse effect increases almost logarithmically with its concentration.
- *Non-Uniform Forcing:* CO_2 radiative forcing is not uniform globally, even if the increase in CO_2 concentration is globally uniform (40). The surface-troposphere radiative forcing (Fig. 4) is a factor of 2 to 3 larger in the tropics (≈ 4.5 W m^{-2}) when compared with the polar forcing (1 to 3 W m^{-2}) and, furthermore, it is larger in summer than in winter (40). The nonlinear increase of the Planck function with temperature, the nonlinear increase in hot bands' absorption coefficient with temperature, and latitudinal variations in cloudiness contribute to the non-uniformity of the forcing.
- *Stratospheric Contribution:* The downward emission from the CO_2 rich stratosphere contributes significantly to the tropopause radiative forcing as shown in Figure 4. In the tropics, this is about 25%, while in the polar regions the stratosphere contributes more than 50%. The increase from tropics towards the poles is due to the factor of 2 increase in the mass of the stratosphere. The increased CO_2 also cools the stratosphere and this decreases the downward emission only slightly (compare the "STRATOSPHERE ΔT=0" curve in Figure 4, which does not account for stratospheric cooling, with the "STRATOSPHERE NFB" curve which does.).
- *Importance of Back Radiation at the Surface:* It is commonly stated that CO_2 absorbs upwelling radiation and then re-emits it to the surface as back radiation. The CO_2 bands overlap with water vapor bands whose opacity is so large that most of the back radiation from CO_2 is absorbed by the intervening layer of H_2O. As a result, the CO_2 back radiation at the surface increases by only 1.2 W m^{-2} (Fig. 3) as opposed to the 4.3 W m^{-2} tropopause radiative forcing.

(ii) Response at t = t_0+ few months: The stratosphere cools and comes into a new radiative equilibrium with the CO_2 rich atmosphere, which reduces the increased downward emission at the tropopause by a few tenths of W m^{-2} (Fig. 3). The Q after the stratosphere has adjusted is:

$$Q\ (t = t_0 + \text{few months}) \approx 4.2\ \text{W m}^{-2}$$

This adjusted forcing is the number used in most assessments (including IPCC).

(iii) Response at t = t_0+ decades: The surface-troposphere will warm until the entire system reaches a new equilibrium, i.e., Q ≈ 0 again. The magnitude of the warming is governed by the rate of heat loss per degree increase in T_s, $\lambda = -\partial Q/\partial T_s$. λ is referred as the feedback factor since it is governed by feedback processes involving water vapor, clouds, ice and snow, ocean-atmosphere dynamics (to mention a few of the possibilities). λ is positive, since Q decreases with an increase in T_s to restore energy balance. We now have, for any time after t_0, $Q(t) = 4.2 - \lambda\ [\ Ts\ (t) - Ts\ (t = t_o)]$. T_s will increase until, Q = 0 again, such that from the above equation, we have for the equilibrium warming ΔT_s

$$\Delta T_s\ (2\ CO_2) = 4.2 / \lambda$$

For the simplest of all possible responses, S, the solar absorption does not change and F can be expressed as black-body emis-

sion, i.e. $F = \sigma T_e^4$, where T_e, the effective emission temperature, is 255 K; such that: $\lambda = -\partial Q/\partial T\sigma = 4\ sT_e^3 = 3.8$ W m^{-2} K^{-1}. For this simple system, devoid of all feedbacks except black-body emission, the magnitude of the warming is 1.1 K. If we next consider the realistic case of atmospheric emission happening in discrete spectral bands (Fig. 2), λ reduces to about 3.3 W m^{-2} K^{-1} and the surface warming is:

$$\Delta T_s\ (2\ CO_2) = 4.2 / 3.3 = 1.3\ K$$

If we now fix the relative humidity, the absolute humidity will increase with an increase in T_s which enhances the water vapor greenhouse effect, and causes a further reduction in OLR. For this case, λ reduces to 2 W m^{-2} K^{-1} and the surface warming becomes 2 K (4.2/2.).

In order to understand why the water vapor must increase, we have to consider global H_2O balance, which, requires consideration of surface energy balance.

Surface Energy Balance and the Hydrological Cycle

The warmer surface (mainly the oceans) evaporates more moisture. Globally, evaporation from the surface must balance precipitation in the atmosphere, and hence precipitation also increases. In this process, the latent energy contained in the H_2O molecule is exported from the surface (so-called evaporative cooling) to the atmosphere (so-called latent heating).

The surface energy balance consists of radiative (R), evaporative (E) and sensible (h) fluxes at the surface. The radiative heating at the surface, in turn consists of 3 components: R = solar absorption + back radiation, i.e. downward emission from the troposphere to the surface—upward emission. The sensible heat flux denotes the vertical exchange of heat between the surface and the atmosphere by boundary layer turbulence and by tropospheric convection. For energy balance, the net heating at the surface, $Q_s = R - (E+h) = 0.0$.

The global E+h is determined by the net radiative heating, R. Thus, if R is increased by CO_2 increase, E+h must also increase. We will illustrate the principles of surface-energy adjustment, from the thought experiment described earlier. Figure 3 illustrates results from a 1-D radiative-convective model (38) that explicitly allowed for moisture balance and the surface energy balance in a radiative convective model. This study (38) identified four separate processes.

Process (I): Out of the 4.2 W m^{-2} of CO_2 forcing, only about 1.2 W m^{-2} is deposited at the surface as increased emission from CO_2, and the balance of 3 W m^{-2} is trapped in the troposphere (Fig. 3). Hence, Qs ($t = t_0$) = 1.2 W m^{-2}.

Process (II): The 3 W m^{-2} direct CO_2 heating of the troposphere warms the troposphere, which radiates some of the energy to the surface and contributes to an additional increase of 2.3 W m^{-2} in the downward emission to the surface. From (I) and (II), $Q_s \approx 3.5$ W m^{-2}, and the surface temperature will increase in response to this heating. R should decrease and/or E and h must increase to balance this net heating:

$$\Delta R - \Delta\ (E+h) + 3.5 = 0.0$$

Process (III): The surface longwave emission increases at a rate of about 5.5 W m^{-2} K^{-1}; but the back radiation also increases correspondingly because of the increase in atmospheric temperature and also because the emissivity of the water vapor and clouds is close to a black body (about 0.9). As a result the net (up minus down) increase in longwave emission is small (only about 10% of the increase in up emission) and R can not compensate for the 3.5 W m^{-2} heating. E and h must increase to restore energy balance. This in turn increases the latent and sensible heating of the troposphere, and the back radiation increases further from the tropospheric warming.

Process (IV): The tropospheric humidity q increases because of two reasons: *i)* increase in evaporation from the surface; and *ii)* because of the exponential increase in saturation vapor pressure with T, the atmosphere holds more vapor with a warming. Observations of the atmospheric humidity profile as a function of latitude and season suggest that the atmosphere tends to conserve its relative humidity with a change in temperature (6, 10); as a result, the absolute humidity is determined by the saturation vapor pressure, which increases by about 6% near the surface to about 10 to 15% in the troposphere per degree rise in temperature. Atmospheric dynamics play a fundamental role in determining the vertical profile of relative humidity. Dynamics is also the underlying reason why the relative humidity profile is invariant with latitude and season (see Bengtsson (36)). The enhanced water vapor increases the back radiation such that R increases ($\Delta R > 0$). The radiative adjustment adds to the net heating instead of decreasing it, thus providing a positive feedback. Thus E+h must increase even more to restore the balance. Since E is larger than h by a factor of 5 to 6, the primary source for restoration of energy balance is the increase in evaporation, which is discussed next.

The saturation specific humidity near the sea surface, according to the Clausius-Clapeyron law, increases by about 6% per degree increase in T. As a result, if the atmospheric humidity and surface wind are held fixed, the surface evaporation will initially increase at a rate given by: dE/dT ≈ 15 to 20 W m^{-2} K^{-1} (38). The obvious consequence of such a large initial increase in evaporation is an increase in humidity in the air above, q_a. In addition, latent heating (LH) of the troposphere will increase since ($\Delta E = \Delta LH$), creating a feedback loop between E, LH and T. The final increase in q_a and tropospheric humidity will be determined by energy balance requirements, since E+h must balance R. This aspect of the energy balance is described in greater detail with a realistic boundary layer physics in (41).

In the Ramanathan model (38) shown in Figure 3, the back radiation increases by 15.5 W m^{-2} (which includes the 1.2 W m^{-2} due to direct CO_2 emission); the up emission increases by 11.5; E+h increases by 4 W m^{-2}. Thus the largest effect of enhancement in atmospheric greenhouse effect is an increase in back radiation by about 7 W m^{-2} per degree increase in Ts. The next big change is an increase in evaporation by about 2 to 4% (1.5 to 3 W m^{-2} K^{-1}) per degree warming.

Solid to liquid and vapor: Ice-albedo feedback The surface warming can melt the sea ice and snow cover. The underlying surface, be it ocean or land, is much darker than the ice or snow, such that it absorbs more solar radiation, thus amplifying the initial warming. The ice-albedo feedback amplifies the global warming by only 10 to 20% (e.g. 13, 14); near the sea-ice margins and in polar oceans, the warming can be much larger.

Sequestering of Heat in the Ocean

The feedbacks influence the rate of storage of the heating in the ocean in an important way. The time dependent form of the ocean-troposphere energy budget is:

$$C\frac{dT}{dt} = 4.2 - \lambda\frac{dT}{dt}$$

where C is the heat capacity of the ocean-atmosphere system. The solution of the transient response is:

$$T(t) = \frac{4.2}{\lambda}\{1. - e^{-\frac{t}{\tau}}\};\ \tau = \frac{C}{\lambda}$$

τ is the *e*-folding response time of the coupled linear system. It is clearly seen that the smaller the feedback factor λ, the greater is the equilibrium warming ($t >> \tau$); but it takes longer to reach equilibrium, since the response time τ increases with a decrease in λ. For an ocean mixed layer of 100 m thick, C ≈ 4 x

10^8 J m^{-2} K^{-1} and for λ = 2 W m^{-2} K^{-1} (yielding 2K for CO_2 doubling), τ is about 2500 days; for a λ closer to the GCM value of 1 W m^{-2} K^{-1} (yielding 4K warming for CO_2 doubling), τ increases to 5000 days.

As a caveat, the system we considered up to this point to elucidate the principles of warming is a highly simplified linear system. Its use is primarily educational and cannot be used to predict actual changes.

PHYSICS OF RADIATIVE FORCING BY NON-CO_2 TRACE GASES

The Atmospheric "Window"

Reverting back to Figure 2, we note that the maximum energy emitted into space is contained in the 8–13 μm region. This is the primary spectral region through which the surface and clouds ventilate heat directly to space. The unpolluted atmosphere is quite transparent in this so-called "window region", except for ozone absorption in the 9.6 μm region. Almost all synthetic gases emitted into the atmosphere have strong absorption bands in the window region as shown in Figure 5. The infrared absorption by these gases literally has the effect of "dirtying" the spectral window of the atmosphere.

CFCs: As pointed out by Ramanathan (17), increasing the concentration of CFC-11 and CFC-12 from 0 to 1 ppbv leads to a surface warming of about 0.13K and 0.15K respectively in a radiative-convective model (17, 20). Comparing this with a surface warming of about 2K (estimated with the same climate model as that used in the CFC estimates) for CO_2 increase from 300 to 600 ppm, it is seen that the addition of one molecule of CFC-11 and CFC-12 can have the same warming effect as adding more than 10^4 molecules of CO_2. CFCs are very effective in enhancing the greenhouse effect because: *i)* CFC-11 and 12 absorb very strongly in the 7–13 ∝m spectral window region and furthermore, between them, there are 5 very strong bands at 9.1 ∝m, 8.7 ∝m, 10.9 ∝m, 9.2 ∝m and 11.8 ∝m; *ii)* the band strengths (wavelength integrated absorption coefficient) are about 5 to 10 times stronger than that of CO_2 (Fig. 5); and *iii)* their present-day concentrations are low enough that their greenhouse effect increases linearly with their concentrations, while the CO_2 effect increases logarithmically.

Comment on IPCC CFC Forcing: The IPCC (1) uses the radiative forcing due to CFC-11 increase from 0 to 1 ppb as a standard for assessing the forcing due to all other non-CO_2 trace gases. The recommended value used by IPCC is 0.2 W m^{-2}. The latest study by Pinnock et al. (42), which employs recent spectroscopic data, obtained a forcing of 0.27 W m^{-2}, identical to the earlier values reported in Ramanathan (17) and Ramanathan et al. (20). IPCC may have to revise its estimate of CFC forcing upwards by about 30%.

CH_4, N_2O, and tropospheric ozone are the other important greenhouse gases. The sensitivity of the tropospheric heat balance to tropospheric O_3 increase is particularly striking. Although only about 6–14% of the total O_3 lies in the troposphere, its longwave opacity is nearly the same as that of stratospheric O_3. A particular fractional decrease of O_3 in the troposphere has about the same net radiative cooling effect on the troposphere as the same (uniform) fractional decrease in the stratosphere (21, 22).

Nature of Radiative Forcing From the Stratosphere

The stratospheric emission and absorption of longwave radiation make an appreciable contribution to the total greenhouse effect and, furthermore, add a considerable degree of complication to the simplified picture presented earlier. These complications arise because of the increase in temperature with altitude in the stratosphere and the non-uniform ozone-mixing ratio.

Stratospheric Radiation Budget: The hemispherical and annual mean values are shown in Figure 6. The hemispherical mean absorption and emission are almost equal; in other words, the stratosphere is essentially in radiative equilibrium. The relative roles of O_3 versus $CO_2 + H_2O$ in the overall energy balance are shown on the bottom left side of Figure 6. O_3 causes a net radiative heating of about 15.5 W m^{-2}, which is compensated by the net cooling due to $CO_2 + H_2O$. The net effect of the stratosphere is to warm the troposphere by about 10.2 W m^{-2}, with the stratospheric O_3 contributing about 2.3 W m^{-2} (bottom center and right side of Fig. 6).

CO_2 Induced Stratospheric Cooling: A Clarification: It is well known that increased CO_2 cools the stratosphere (e.g. 10). The standard explanation given is that this cooling is due to the increase in the longwave emission to space by stratospheric CO_2. In a very fundamental sense this explanation is inadequate and possibly misleading (Prof. David Rogers alerted me to this inadequacy; see Hartmann (43) for a mathematically correct explanation). The magnitude as well as the sign of the temperature change depends on the temperature profile. As we mentioned earlier, in our explanation of the greenhouse effect, OLR reduces (with an increase in CO_2) because of the decrease in temperature with altitude. In the stratosphere, however, temperature increases with altitude and as a result the cooling to space is larger than the absorption from layers below. This is the fundamental reason for the CO_2 induced cooling. Since ozone radiative (solar and 9.6 μm longwave) heating is the primary reason for the increase of temperature with altitude, the effect of CO_2 on

Figure 5. Spectral locations of the absorption features of various trace gases. The spectral region between 7 and 13 Êm is referred to as the atmospheric "window." Abbreviations: F denotes CFC; PAN denotes peroxyacetyl nitrate; and STP, standard temperature and pressure.

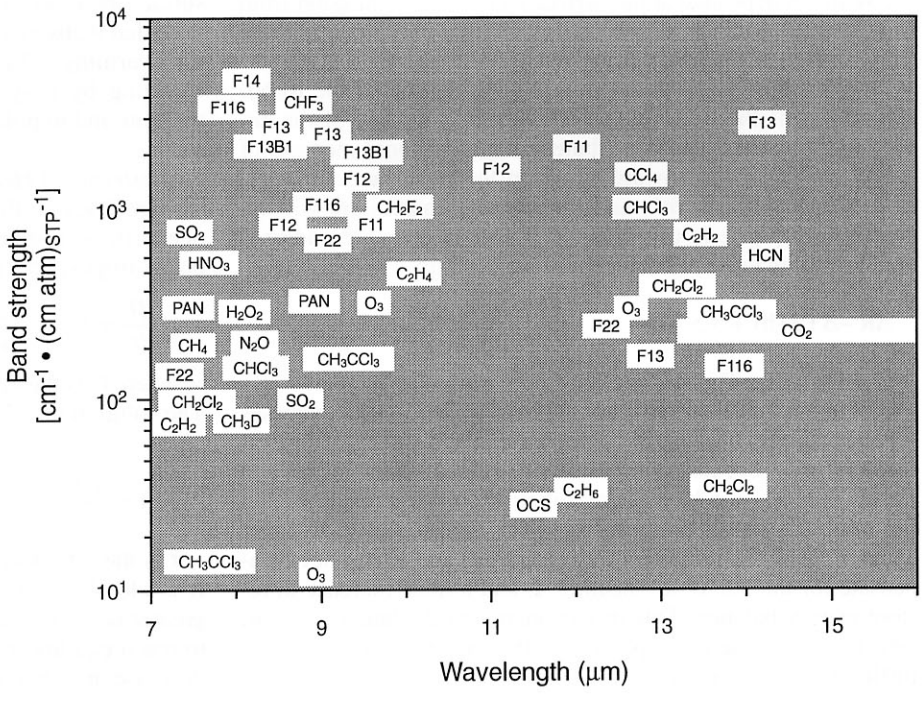

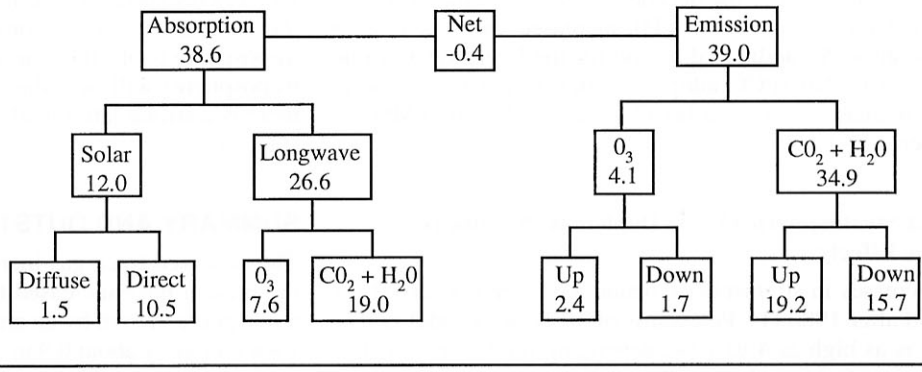

Relative Effects of 0_3 and $C0_2 + H_20$ in the Stratosphere.	Stratospheric Effect on the Tropospheric Energy Balance (a) Total		(b) 0_3	
0_3(=12.0 + 7.6 - 4.1) = 15.5	Solar = -10.5 x 0.69 = -7.2		Solar =	-7.2
$C0_2 + H_20$(=19.0-34.9) = -15.9	IR =	17.4	Longwave, 0_3 =	1.7
	Net = (17.4 - 7.2)	10.2	Longwave, ($C0_2 + H_20$) =	7.8 (15.7/2)
			Net	2.3

Source: Ramanathan and Dickinson (21)

Figure 6. Global mean stratosphere radiative energy balance. Net = absorption – emission. Units W m^{-2}. Source: (21)

stratospheric temperatures will depend on the ozone levels in the stratosphere.

Stratospheric Ozone Decrease: A decrease in stratospheric O_3, irrespective of the altitude of that decrease, would lead to an increase in the solar radiation reaching the troposphere, and this solar effect would tend to warm the surface. However, O_3 also alters the IR (longwave) emission from the stratosphere in two ways; first, the decreased solar absorption (due to O_3 decrease) cools the stratosphere; the cooler stratosphere emits less downward to the troposphere. Second, a decrease in O_3 reduces the absorption (by the O_3 9.6-μm band) of the surface-troposphere emission. This reduction causes an additional cooling of the stratosphere, which in turn, causes an additional reduction in the downward IR emission by the stratosphere. Thus, the IR effects of O_3 decrease tend to cool the surface.

The surface warming induced by the solar effect is independent of the altitude of O_3 perturbation. On the other hand, the IR effect (of stratospheric cooling) on the troposphere increases with a decrease in the altitude of ozone depletion. Consequently, for a decrease in the upper stratosphere O_3, the solar effect dominates, leading to a surface warming, while for a decrease in the lower stratosphere O_3, the IR effect dominates, leading to a surface cooling (12, 21). In summary, the effect of stratospheric ozone decrease depends very strongly on the altitude of ozone decrease (12, 21, 29, 44).

TRACE-GAS RADIATIVE FORCING SINCE THE PRE-INDUSTRIAL ERA

Direct Greenhouse Effect

It is convenient to consider 4 separate periods during the post-industrial era: *i)* Pre-1850s, when the anthropogenic emissions of trace gases were negligible; *ii)* 1850 to 1960, when CO_2 effects were dominant; *iii)* 1960 to 1980s, when the non-CO_2 trace gas effects were becoming comparable to the CO_2 radiative forcing, and the effects of stratospheric ozone depletion were either small or negligible; and *iv)* 1980s to present, when the stratospheric ozone depletion effects including that of the Antarctic ozone hole were potentially large.

Table 2 lists the observed trace-gas changes and the calculated forcing for pre-1850 to 1980 from the WMO assessment report by Ramanathan et al. (27). Also shown in Table 2 are IPCC values for the 1850 to 1990 period. Major conclusions from the Table are:

- For the entire period 1850 to 1980, non-CO_2 trace gases contributed about 35% and CO_2 about 65% to the total greenhouse effect.
- For the 1960 to 1980 period however, the non-CO_2 greenhouse effect (not shown here) rivaled that of CO_2 (27). Prior to 1960s, contributions from gases such as CFCs (and other Halons) and Ozone were much smaller. Thus, there was a fundamental change in the composition of the greenhouse effect after the 1850–1960 period.
- The rate of decadal CO_2 plus non-CO_2 forcing (W m^{-2} per decade) increased dramatically with time. For example, the forcing during the 1980s was about a factor of 3 larger when compared with the average rate of decadal increase for the 1850 to 1960 period.

Table 2. Comparison of estimated radiative forcing due to direct radiative effects of greenhouse gases. (Source:[1] WMO Assessment Report (27) ; [2]IPCC (1)).
Does not Include effects of Stratospheric Ozone decrease and aerosols

Trace Gas	Surface-Atmosphere Radiative Forcing	
	Pre 1850–1980[1]	Pre 1850–1994[2]
CO_2	1.1	1.56
CO_2 plus all other trace gases without tropospheric Ozone	1.83	2.85

Adopted Concentration Changes

Trace Gas	Concentration Change	
	Pre 1850 to 1980	Pre 1850 to 1994
CO_2 (ppmv)	275–339	278 to 358
CH_4 (ppmv)	0.7–1.7	0.7 to 1.72
N_2O (ppmv)	0.285–0.3	0.275 to 0.310
CFC11 (ppbv)	0–0.18	0. to 0.268
CFC 12(ppbv)	0–0.28	0. to 0.503
All other halons	See Table 1 in (20)	See Table 2.1, IPCC (1)
Trop Ozone	12.5% change from 0 to 12 km	About 50%

– Thus, the inclusion of the decade of 1980s (see the third column in Table 2 from IPCC (1)), increased the total forcing significantly. An additional reason for the larger IPCC value (Table 2) is that IPCC adopts a much larger tropospheric ozone increase (≈ 50% in IPCC versus 12.5% in WMO assessment (27)).

Effects of Stratospheric Ozone Depletion: Nonlinear Radiative Effects

Large decreases in stratospheric ozone have been observed for the period after 1980 (1). Polewards of 40 N the decadal rate of decrease is as high as 4 to 10%, depending on the season. The net radiative forcing due to this decrease as estimated by Ramaswamy et al. (29) has a hybrid structure with relatively smaller changes in the equatorial regions and a large net cooling in the polar regions, with a maximum in the southern polar spring time. As shown by Ramanathan and Dickinson (21), even for the same percent decrease at all altitudes and all latitudes, the net cooling effect at the tropopause increases from equator towards the poles with maximum cooling during polar spring (Fig. 7). The negative longwave forcing is larger in the polar regions primarily because more of the ozone resides in the lower stratosphere (see earlier discussion on the altitude dependence of the longwave effect). In the Ramaswamy et al. study (29), the above effects are further amplified by the larger ozone decrease in the polar latitudes. The net global average radiative forcing due to the observed ozone decrease during 1979 to 1990 is estimated to be –0.1 W m^{-2}, while Hansen et al. (45) employ even larger ozone decreases in the lower stratosphere/upper troposphere region and suggest a larger radiative forcing of –0.3 W m^{-2}.

However, the tropopause forcing may not be a reliable index for the climatic effects of stratospheric ozone depletion. The individual values of the two competing effects (see earlier discussions) of solar heating and longwave cooling are factors of 3 to 10 larger than the net effect. The longwave cooling effects are largely concentrated within the upper troposphere. If instead of the standard radiative-convective adjustment, just the upper troposphere cools, then the surface (as well as the lower to mid-troposphere) will be subject to net solar heating. In addition, there is a strong latitudinal and seasonal gradient in the forcing (Fig. 7).

SUMMARY AND OUTSTANDING ISSUES

The observed trace-gas increases from the mid-19th century to the present have increased the radiative heating of the surface-atmosphere system by an amount comparable to a change in the solar output by about 0.9 to 1.2%. During the middle to late 20th century, the non-CO_2 trace gases have added to the radiative heating of the planet by an amount comparable to that of CO_2. CFC increase has been arrested after 1990. By itself, and if not accompanied by other competing changes, this radiative heating should have committed the planet to an eventual warming of about 1 to 1.5 K. Even if the ocean has sequestered 50% of this forcing, the planet should have warmed by about 0.5 to 0.8 K (from the pre-industrial era to now), which is not inconsistent with the observed record (1).

The largest effect of global warming on the energy budget is an enhancement of the back radiation from the warmer surface-atmosphere system. For example, a 2 K warming in response to a doubling of CO_2 would increase the back radiation at the surface by about 12 to 14 W m^{-2}, and only about 1 W m^{-2} is due to the direct radiative effect of CO_2 doubling. This has important consequences for how the surface energy budget and the hydrological cycle would respond. Our ability to predict such regional climate effects, depends critically on resolving a number of outstanding issues, described below.

Aerosol Forcing

The radiative forcing of anthropogenic (sulfates, smoke, dust and organics) aerosols must rank as the most significant uncertainty in our understanding of the anthropogenic forcing. These solar

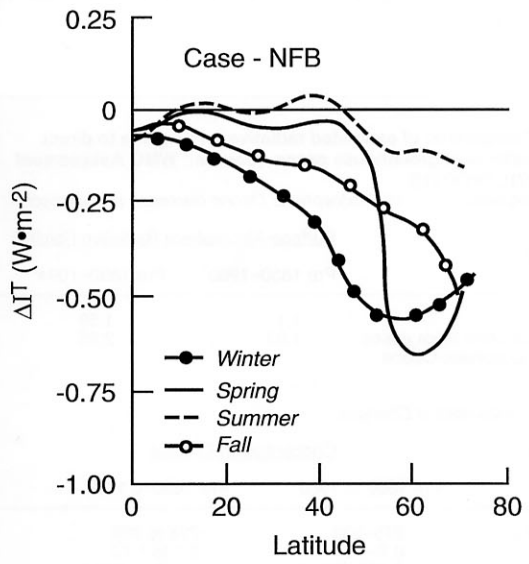

Figure 7. Seasonal change in the tropospheric radiative energy input for a 30% uniform reduction in stratospheric O_3. $D\Delta I^T$ is the radiative forcing of the tropopause. Stratospheric temperature changes are adjusted from observed values by assuming radiative equilibrium.

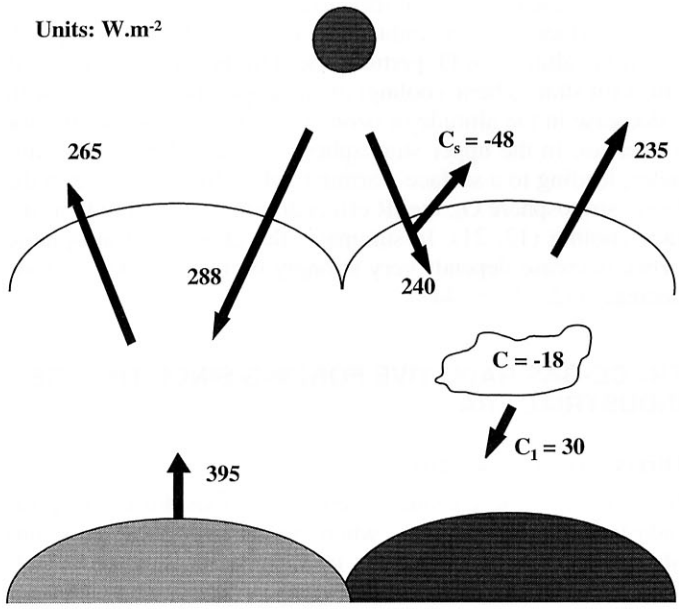

Figure 8. Global average clear sky radiation budget (left panel) and average cloudy fluxes and cloud radiative forcing (right panel) from ERBE. Unless otherwise marked, outgoing arrows denote OLR and incoming arrows denote net incoming solar. Uncertainties in these fluxes are ± 5 W m^{-2} and in cloud forcings these uncertainties are about ± 7 W m^{-2}. The values are for 5 yr averages between 1985 and 1989. Source: (33, 34).

cooling effects are concentrated regionally (Northern Hemisphere mid-latitude regions, tropical rainforest regions and in Asia). It is not clear whether the climate system responds to these regional radiative forcings on global or regional scales.

Excess Solar Absorption in Cloudy Skies

How much solar radiation is absorbed in the clear and cloudy atmosphere? Current wisdom is that, globally, about 20% is absorbed within the atmosphere (including cloudy regions) and 50% is absorbed at the surface (IPCC (1)). Several recent studies (46–49) using observational data from satellites, surface and aircraft, concluded that the atmospheric absorption in average cloudy skies is as much as 28% (or 25 W m^{-2} globally), and the surface absorption correspondingly smaller by about 8%, i.e., 42% instead of 50%; thus resurrecting the controversy of the 1960s and 1970s when it was indicated that observed absorption almost always exceeded theoretical values (7, 50). Furthermore, three of the recent studies (46–48) conclude that most if not all of the excess absorption is in cloudy skies. The issue remains controversial because, other recent aircraft data (51) do

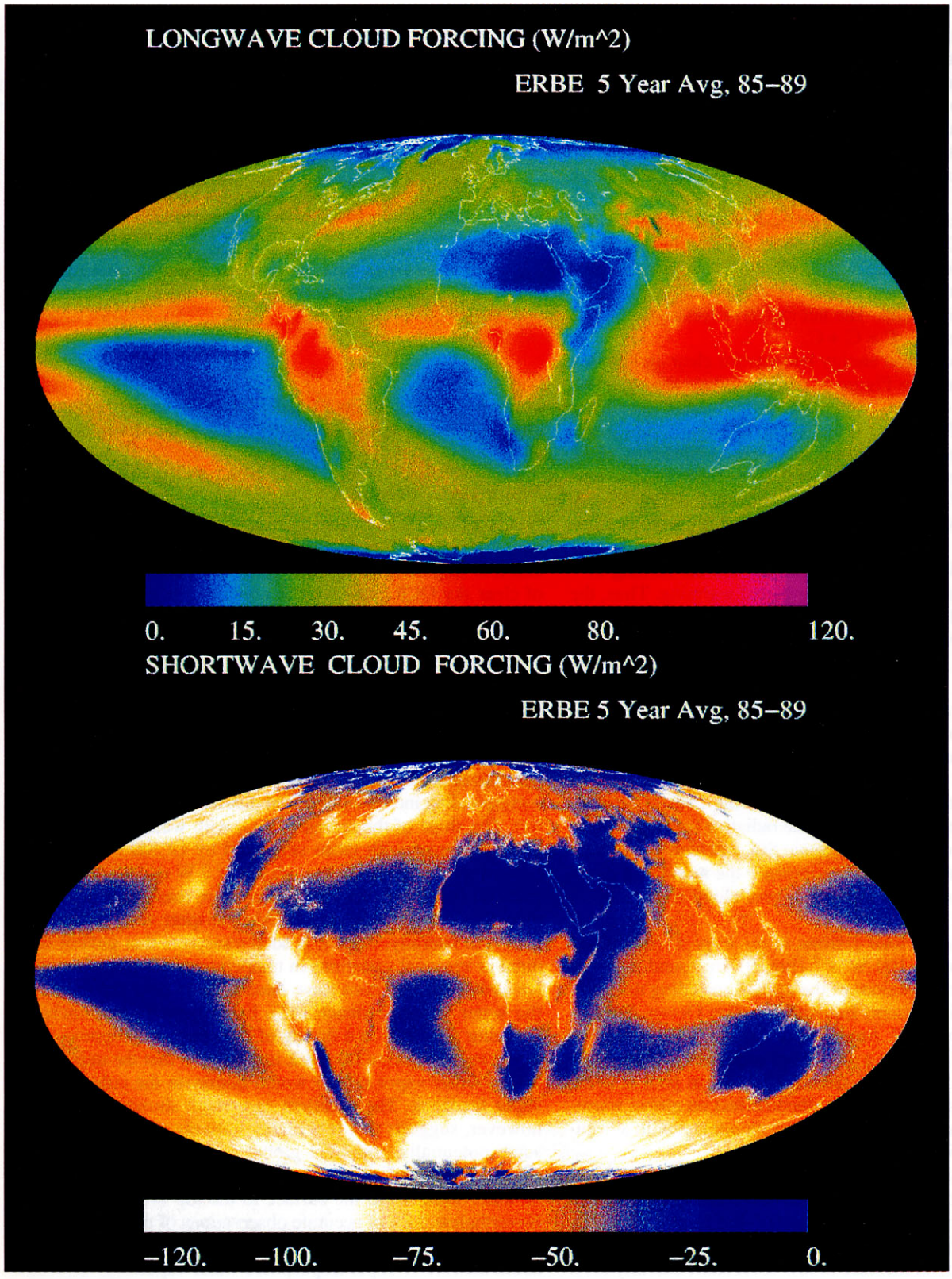

Figure 9. Five-year (1985 to 1990) averages of ERBE regional longwave (top panel) and short wave cloud forcing (bottom panel) from data described in Ramanathan et al. (33) and Harrison et al. (34).

not reveal as much excess absorption. If the recent studies are confirmed, then our estimates of surface evaporation, sensible heat fluxes and longwave radiation (since globally, the sum of these 3 components have to balance solar absorption at the surface) have to be revised accordingly with potentially important implications for our understanding of the hydrological cycle.

Clouds

Do Clouds Heat or Cool the Planet? Until the advent of satellite radiation budget experiments in the late 60s, model studies were the main source of insights into the global radiative effects of clouds (10, 52). These and more recent GCM studies (13, 14, 36) suggested that clouds have a large net radiative cooling effect on the planet. The Earth Radiation Budget Experiment, ERBE (53), using the so-called cloud forcing approach (33), settled the issue of whether clouds have a net global heating or cooling effect on the present day climate (33, 34). ERBE separated the clear-sky radiation budget from the radiation budget of average cloudy skies. The difference in the radiation budget between the clear and average cloudy skies yielded the cloud radiative forcing.

The longwave cloud forcing, C_l = Fc-F, where F and Fc are, respectively, the OLR for average clear and cloudy skies. The shortwave cloud forcing, C_s = S (1 -A) -S (1 -Ac), where S is the solar insolation at TOA, A and Ac are the column albedos for average and clear skies. The net radiative forcing of clouds is given by the sum, i.e., $C = C_l + C_s$.

The 5-year global mean energy budgets for clear and cloudy regions are illustrated in Figure 8. Clouds reduce the absorbed solar radiation by 48 W m^{-2} (C_s = -48 W m^{-2}) while enhancing the greenhouse effect by 30 W m^{-2} (C_l = 30 W m^{-2}), and therefore clouds cool the global surface-atmosphere system by 18 W m^{-2} (C = -18 W m^{-2}) on average. The mean value of C is several times the 4 W m^{-2} heating expected from doubling of CO_2 and thus the earth would probably be substantially warmer without clouds.

Cloud Feedback: We do not know how the net forcing of –18 W m^{-2} will change in response to global warming. Thus, the magnitude as well as the sign of the cloud feedback is uncertain. Cloud radiative forcing effects are concentrated regionally (Fig. 9). The data reveal 3 regions of major interest for future study.

a) Storm track cloud systems over mid-latitude oceans: These cloud systems associated with extra tropical cyclones along with the persistent oceanic stratus, reflect more that 75 W m^{-2} of solar radiation (Cs < –75 W m^{-2}), and contribute about 60% of the –18 W m^{-2} net global cloud radiative forcing (54). Anthropogenic activities can directly perturb the radiative forcing of these clouds. The emission of anthropogenic SO_2 and their subsequent conversion to sulfate aerosols can increase the number of cloud drops, which can enhance the short-wave cloud forcing by as much as –5 to –10 W m^{-2} (31).

ii) Deep convective cloud systems in the tropics: Maxima in C_l and in $-C_s$ of 60 to 100 W m^{-2} (Fig. 9) are found over the convectively disturbed regions of the tropics, including the tropical Western Pacific, Eastern Equatorial Indian Ocean, Equatorial rainforest regions of S. America and Africa. These cloud systems have been linked with a number of important climate feedback effects including the Western Pacific warm pool convective-cirrus thermostat (55), cirrus albedo effect on global warming (56) and increased convective-cirrus cloudiness with a tropical warming (57, 58).

iii) Marine stratocumulus coastal and sub-tropical cloud systems: These sub-tropical cloud systems also contribute more than 75 W m^{-2} to $-C_s$ and extend as far as 1000 km from the western coasts of N. America, S. America, and S. Africa. Cloudiness is shown to increase with increase in low-level static stability (59).

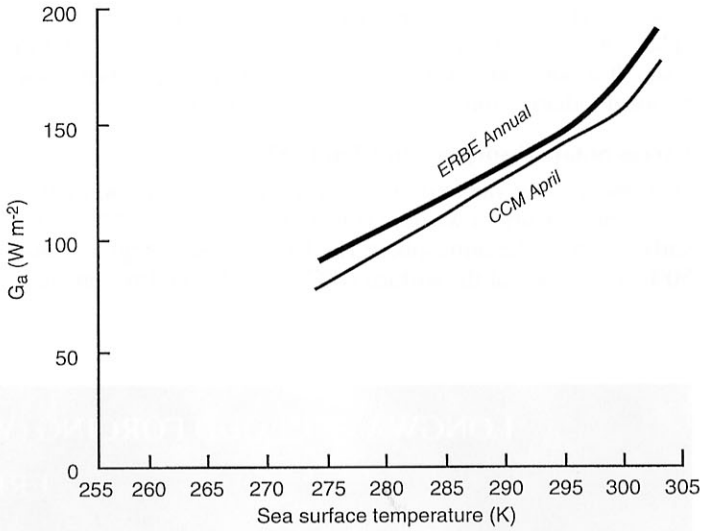

Figure 10. Comparison of G_a and sea surface temperature, obtained from two sources: bold line, ERBE annual values, obtained by averaging April, July and October 1985 and January 1986. Uncertainty in G_a is ± 10 W m^{-2}; thin line, three-dimensional climate-model simulations for a perpetual April. CCM denotes National Center for Atmospheric Research, Community Climate Model. The results shown above were obtained from CCM version O, developed 15 years ago. Adapted from Raval and Ramanathan (60).

Furthermore, the effects of sulfate aerosols in enhancing cloud albedo are expected to be large for these low level cloud systems.

Water Vapor Feedback

Nearly all GCMs show that increases in surface and tropospheric temperatures lead to an increase in water vapor concentration and it is important to test this feedback with data. Availability of clear sky OLR enables us to compute the column integrated (from the surface to the top-of-the atmosphere) atmospheric greenhouse effect (G_a) directly (60), as the difference between surface emission and clear sky OLR. From Figure 8, the global G_a is 130 W m^{-2} (395–265) with a 2σ uncertainty of ± 10 W m^{-2}. When the longwave cloud forcing is added to G_a, we obtain the total greenhouse effect of the atmosphere and clouds. The data show that G_a increases from pole to equator, largely because of increase in surface-troposphere temperature, and the corresponding increase in vertical distribution of water vapor (60, 61). The slope of the increase of G_a with water vapor and temperature agrees with those simulated by GCMs (Fig. 10), and furthermore it is consistent with a λ of 2 W m^{-2} K^{-1} (see discussions on feedback). Such agreements are reassuring in that they give confidence in the way GCMs transport water vapor vertically and laterally, since it is such transports that govern latitudinal or seasonal variations in temperature, water vapor and G_a. Nevertheless, questions have been raised about the validity of the water vapor feedback (62), by suggesting that increased warming may lead to a drying of the upper troposphere, exerting a strong negative feedback instead; and that the upper troposphere water-vapor effects would dominate the column water-vapor feedback. The excellent agreement shown in Figure 10, however, suggests that it is highly unlikely models are missing some potentially important global scale water-vapor transport effects, particularly because G_a includes the greenhouse effect of water vapor from the surface to the top of the stratosphere. Nevertheless, lack of accurate observations of upper troposphere water vapor, preclude us from making any definitive statement about the role of upper troposphere water vapor.

References

1. IPCC. 1995. Climate Change 1995, The Science of Climate change, Contribution of working group I. Intergovernmental Panel on Climate Change. Houghton, J.T., Meira Filho, L.G., Callandar, B.A., Harris, N., Kattenberg, A. and Maskell, K. (eds). Published by the Cambridge University Press, pp. 572.
2. Fourier, B.J.B. 1827. Memoire sur les temperatures du globe terrestre et des espaces planetaires. *Mem. R. Sci. Inst. France 7*, 572–604.
3. Pouillet, M. 1838. Memoire sur la chaleur solair, sur les pouvoirs rayonnants et absorbants de l'air atmospherique, et sur la temperature de l'espace. *Comptes Rendus Seances Acad. Sci.* 24–76.
4. Tyndall, J. 1863. On radiation through the earth's atmosphere. *Proc. Roy. Inst.,* Jan. 23, 1863, 200–206.
5. Langley, S.P. 1889. The temperature of the moon. *Mem. Natl. Acad. Sci. 4*, Part II, 107–212.
6. Arrhenius, S. 1896. On the influence of carbonic acid in the air upon the temperature of the ground. *Philos. Trans. 41*, 237–276.
7. Ramanathan, V. and Vogelman, A.M. 1997. Greenhouse effect, atmospheric solar absorption and the Earth's radiation budget: From the Arrhenius/Langley era to the 1990s. *Ambio 26*, 38–46.
8. Chamberlin, T.C. 1897. An attempt to form a working hypothesis of the cause of glacial periods on an atmospheric basis. *J. Geology. 7*, 545.
9. Callendar, G.S. 1938. The artificial production of carbon dioxide and its influence on temperature. *Quart . J. Roy. Met. Soc. 64*, 223–240.
10. Manabe, S. and Wetherald, R.T. 1967. Thermal equilibrium of the atmosphere with a given distribution of relative humidity. *J. Atmos. Sci. 24*, 241–259.
11. Ramanathan, V. and Coakley, Jr., J.A. 1979. Climate modeling through radiative-convective models. *Rev. Geophys. Space Physics. 16,* 465-489.
12. Ramanathan, V., Callis, L.B. and Boughner, R.E. 1976. Sensitivity of surface temperature and atmospheric temperature to perturbations in the stratospheric concentration of ozone and nitrogen dioxide. *J. Atmos. Sci. 33*, 1092–1112.
13. Manabe, S. and Wetherald, R.T. 1975. The effects of doubling the CO_2 concentration on the climate of a general circulation model. *J. Atmos. Sci. 32*, 3–15.
14. Hansen, J.E., Lacis, A., Rind, D., Russel, G., Stone, P., Fung, I., Ruedy, R. and Lerner, J. 1984. Climate sensitivity: analysis of feedback mechanisms. In: *Climate Processes and Climate Sensitivity*, Series 5. Clark, W.C. (ed.). New York: Clarendon Press, pp. 284–286.
15. Crutzen, P.J. 197O. SST's: The influence of nitrogen oxides on the atmospheric ozone content. *Quart. J. Roy. Meteorol. Soc. 96*, 320–325.
16. Molina, M.J. and Rowland, F.S. 1974. Stratospheric sink for chlorofluoro-methanes: Chlorine atom catalyzed destruction of ozone. *Nature 249*, 810–812.
17. Ramanathan, V. 1975. Greenhouse effect due to chlorofluorocarbons: climatic implications. *Science 190*, 50–52.
18. Wang, W.C., Yung, Y.L., Lacis, A.A., Mo, T. and Hansen, J.E. 1976. Greenhouse effect due to manmade perturbations to global climate. *Science 194*, 685–690.
19. Donner, L. and Ramanathan, V. 1980. Methane and nitrous oxide: Their effects on the terrestrial climate. *J. Atmos. Sci. 37*, 119–124.
20. Ramanathan, V., Cicerone, R.J., Singh, H.G. and Kiehl, J.T. 1985. Trace gas trends and their potential role in climate change. *J. Geophys. Res. 90*, 5547–5566.
21. Ramanathan, V. and Dickinson, R.E. 1979. The role of stratospheric ozone in the zonal and seasonal radiative energy balance of the earth-troposphere system. *J. Atmos. Sci. 36*, 1084–1104.
22. Fishman, J., Ramanathan, V., Crutzen, P.J. and Liu, S.C. 1979. Tropospheric ozone and climate. *Nature 282*, 818–820.
23. Wang, W.C., Wuebbles, D.J., Washington, W.M., Issacs, R.G. and Molar, G. 1986. Trace gases and other potential perturbations to global climate. *Rev. Geophys. 24*, 110–140.
24. Brühl, C. and Crutzen, P.J. 1987. Scenarios of possible changes in atmospheric temperatures and ozone concentrations due to man's activities as estimated with a one-dimensional coupled photochemical climate model. *Clim. Dynam. 2,* 173–203.
25. Dickinson, R.E. and Cicerone, R.J. 1986. Future global warming from atmospheric trace gases. *Nature 319*, 109–114.
26. Tricot, C. and Berger, A. 1987. Modeling the equilibrium and transient response of global temperature to past and future trace gas concentrations. *Clim. Dynam. 2*, 39–61.
27. Ramanathan, V., Callis, Jr., L.B., Cess, R.D., Hansen, J.E., Isaksen, I.S.A., Kuhn, W.R., Lacis, A., Luther, F.M., Mahlman, J.D., Reck, R.A. and Schlesinger, M.E. 1985. Trace gas effects on climate. In: *World Meteorological Organization Global Ozone Research and Monitoring Project-Report No. 16 Atmospheric Ozone—Assessment of our Understanding of the Processes Controlling its Present Distribution and Change.*
28. Keeling, C.D. 1973. Industrial production of carbon dioxide from fossil fuels and limestone. *Tellus 25*, 174–198.
29. Ramaswamy, V., Schwarzkopf, M.D. and Shine, K.P. 1992. Radiative forcing of climate from halocarbon-induced global stratospheric ozone loss. *Nature 355*, 810–812.
30. Charlson, R.J., Langner, J. and Rodhe, H. 1990. Sulfate aerosol and climate. *Nature 348*, 22.
31. Kiehl, J.T. and Briegleb, B.P. 1993. The relative role of sulfate aerosols and greenhouse gases in climate forcing. *Science 260*, 311–314.
32. Kaufman, Y.J. and Fraser, R.S. 1997. The effect of smoke particles on clouds and climate forcing. *Science 277*, 1636–1638.
33. Ramanathan, V., Cess, R.D., Harrison, E.F., Minnis, P., Barkstrom, B.R., Ahmad, E. and Hartmann, D. 1989. Cloud-radiative forcing and climate: results from the earth radiation budget experiment. *Science 243*, 57–63.
34. Harrison, E.F., Minnis, P., Barkstrom, B.R., Ramanathan, V., Cess, R.D. and Gibson, G.G. 1990. Seasonal variation of cloud radiative forcing derived from the Earth Radiation Budget Experiment. *J. Geophys. Res. 95,* 18687–18703.
35. Cess, R.D. and 31 authors. 1995. Intercomparison and interpretation of climate feedback processes in 19 atmospheric general circulation models. *J. Geophys. Res. 95*, 16601–16615.
36. Bengtsson, L. 1997. A numerical simulation of anthropogenic climate change. *Ambio 26*, 58–65.
37. Hanel, R.A., Conrath, B.J., Kunde, V.G., Prabhakara, C., Revah, I., Salomonson, V.V. and Wolford, G. 1972. The Nimbus 4 infrared spectroscopy experiment 1. Calibrated thermal emission spectra, *J. Geophys Res. 77*, 2629–2641.
38. Ramanathan, V. 1981. The role of ocean-atmosphere interactions in the CO_2 climate problem. *J. Atmos. Sci. 38*, 918–930.
39. Augustsson, T. and Ramanathan, V. 1977. A radiative-convective model study of the CO_2 climate problem. *J. Atmos. Sci. 34*, 448–451.
40. Ramanathan, V., Lian, M.S. and Cess, R.D. 1979. Increased atmospheric CO_2: zonal and seasonal estimates of the effect on the radiation energy balance and surface temperature. *J. Geophys. Res. 84*, 4949–4958.
41. Betts, A.K. and Ridgway, W. 1989. Coupling of the radiative, convective, and surface fluxes over the Equatorial Pacific. *J . Atmos. Sci. 45*, 522–536.
42. Pinnock, S.L., Hurley, M.D., Shine, K.P., Wallington, T.J. and Smyth, T.J. 1995. Radiative forcing of climate by hydrochloroflurocarbons and hydrofluorocarbons. *J. Geophys. Res. 100*, 23227–23238.
43. Hartmann, D.L. *Global Physical Climatology*. 1994. Vol. 56 in International Geophysics Series. Dmowska, R. and Holton, J.R. (eds). Academia Press, San Diego, CA.
44. Lacis, A., Hansen, J., Lee, P., Mitchell, T. and Lebedeff, S. 1981. Greenhouse effect of trace gases. *Geophys. Res. Lett. 8*, 1035–1038.
45. Hansen, J. et al. 1997. Forcings and chaos in interannual to decadal climate change. *J. Geophys. Res. 102* (D22) 25 679–25 720.
46. Cess, R.D. and 20 authors. 1995. Absorption of solar radiation by clouds: Observations versus models. *Science 267*, 496–499.
47. Ramanathan, V., Subasilar, B., Zhang, G.J., Conant, W., Cess, R.D., Kiehl, J.T., Grassl, H. and Shi, L. 1995. Warm pool heat budget and shortwave cloud forcing: a missing physics? *Science 267*, 499–503.
48. Pilewskie, P. and Valero, F.P.J. 1995. Direct Observations of excess solar absorption by clouds. *Science 267*, 1626–1629.
49. Ohmura, A. and Gilgen, H. 1993. Re-evaluation of the global energy balance. *Geophys. Monogr. 75*, IUGG 15, 93–110.
50. Stephens, G.L. and Tsay, S.-C. 1990. On the cloud absorption anomaly. *Q. J. Roy. Met. Soc. 116*, 671–704.
51. King, M.D., Radke, L.F. and Hobbs, P.V. 1990. Determination of the spectral absorption of solar radiation by marine stratocumulus clouds from airborne measurements within clouds. *J. Atmos. Sci. 47*, 894–907.
52. Schneider, S.H. 1972. Cloudiness as a global climate feedback mechanism: The effects of a radiation balance and surface temperature of variations in cloudiness. *J. Atmos. Sci. 29*, 1413–1422.
53. Barkstrom, B.R., Harrison, E., Smith, G., Green, R., Kibler, R., Cess, R. and the ERBE Science Team. 1989. Earth Radiation Budget Experiment (ERBE) archival and April 1985 results. *Bull. Am Meteorol. Soc. 70*, 1254–1262.
54. Weaver, C.P. and Ramanathan, V. 1997. Relationships between large-scale vertical velocity, static stability, and cloud radiative forcing over Northern Hemisphere extratropical oceans. *J. Clim.* 10, 2871–2887.
55. Ramanathan, V. and Collins, W. 1991. Thermodynamic regulation of ocean warming by cirrus clouds deduced from observations of the 1987 el Niño. *Nature 351*, 27–32.
56. Washington, W.M. and Meehl, G.A. 1993. Greenhouse sensitivity experiments with penetrative cumulus convection and tropical cirrus albedo effects. *Climate Dynamics 8*, 211–223.
57. Wetherald, R.T. and Manabe, S. 1988. Cloud feedback processes in a general circulation mode. *J. Atmos. Sci. 45*, 1397–1415.
58. Mitchell, J.F.B. and Ingram, W.J. 1992. Carbon dioxide and climate: Mechanisms of changes in clouds. *J. Climate 5*, 5–21.
59. Klein, S. and Hartmann, D.L. 1993. The seasonal cycle of low stratiform clouds. *J. Climate 6*, 1587–1606.
60. Raval, A. and V. Ramanathan, 1989. Observational determination of the greenhouse effect. *Nature 342*, 758–761.
61. Stephens, G.L. and Greenwald, T.J. 1991. The earth's radiation budget and its relation to atmospheric hydrology. 1. Observations of the clear sky greenhouse effect. *J. Geophys. Res. 96*, 15311–15324.
62. Lindzen, R.S. 1990. Some coolness concerning global warming. *Bull. Amer. Meteor. Soc. 71*, 288–299.

63. Acknowledgments. I thank the Volvo Foundation for the honor. This paper was written while the author was visiting the NASA-Goddard space flight center and I thank Drs. Yoram Kaufman and M. King for hosting me. Numerous colleagues contributed to the work described here and I thank in particular, Drs: B. R. Barkstrom, R. D. Cess, W. D. Collins, P. J. Crutzen, E. A. Frieman, J. T. Kiehl, J. Kuettner and C. Weaver. I thank Drs. L. Bengtsson and K. Noone for their detailed comments on this paper. This work was funded by NSF, NASA and DOE. This is publication #187 from the Center for Clouds, Chemistry and Climate.

V. Ramanathan is Director of the Center for Atmospheric Sciences and the Center for Clouds, Chemistry and Climate at the Scripps Institution of Oceanography, University of California at San Diego. He is professor of atmospheric sciences and Victor C. Alderson Professor of Applied Ocean Sciences. His primary interests are in global warming, earth radiation budget, and clouds and water vapor feedback. He is co-recipient of the 1997 Volvo Environment Prize and received the Buys Ballot Medal for the decade of 1985-1995. He is a member of the American Academy of Arts and Sciences and Academia Europaea. His address: Center for Clouds, Chemistry and Climate, Scripps Institution of Oceanography, University of California at San Diego, 9500 Gilman Drive, La Jolla, CA 92093-0221, USA. e-mail: ram@fiji.ucsd.edu